

A smartphone application to detection and classification of coffee leaf miner and coffee leaf rust

Giuliano L. Manso^a, Helder Knidel^a, Renato A. Krohling^{a,b,c}, José A. Ventura^d

^a*Labcin - Laboratory of Computing and Engineering Inspired by Nature, UFES - Federal University of Espírito Santo, Vitória, Brazil*

^b*PPGI - Graduate Program in Computer Science, UFES, Vitória, Brazil*

^c*Production Engineering Department, UFES, Vitória, Brazil*

^d*Incapar, Rua Afonso Sarlo, 160, Bento Ferreira, 29052-010 Vitória, ES, Brazil*

Abstract

Generally, the identification and classification of plant diseases and/or pests are performed by an expert. One of the problems facing coffee farmers in Brazil is crop infestation, particularly by leaf rust *Hemileia vastatrix* and leaf miner *Leucoptera coffeella*. The progression of the diseases and or pests occurs spatially and temporarily. So, it is very important to automatically identify the degree of severity. The main goal of this article consists on the development of a method and its implementation as an App that allow the detection of the foliar damages from images of coffee leaf that are captured using a smartphone, and identify whether it is rust or leaf miner, and in turn the calculation of its severity degree. The method consists of identifying a leaf from the image and separates it from the background with the use of a segmentation algorithm. In the segmentation process, various types of backgrounds for the image using the HSV and YCbCr color spaces are tested. In the segmentation of foliar damages, the Otsu algorithm and the iterative threshold algorithm, in the YCgCr color space, have been used and compared to *k-means*. Next, features of the segmented foliar damages are calculated. For the classification, artificial neural network trained with extreme learning machine have been used. The results obtained shows the feasibility and effectiveness of the approach to identify and classify foliar damages, and the automatic calculation of the severity. The results obtained are very promising according to experts.

Keywords: Segmentation, Feature extraction, Artificial neural networks, Extreme learning machine, Coffee leaf Rust, Coffee leaf miner, *Hemileia vastatrix*, *Leucoptera coffeella*.

1. Introduction

Plant diseases [1] are usually caused by microorganisms, such as bacteria, fungi, nematodes and viruses, but may still be caused by lack or excess of: 1) essential nutrients for the growth of plants, 2) water and 3) light. In this case, they are also known as physiological disorders. There are many measures that can be taken to avoid the occurrence of disease or even reduce its impact. The observation of a set of control measures and early identification reduce the chance of economic losses with the production and also the use

of chemicals products. So, the automatic identification of the diseases and pests are desirable to the health of a plantation. Diseases can affect plants to varying degrees, from small damages until the annihilation of the plantation as a whole. Coffee leaf rust caused by the fungus *Hemileia vastatrix*, is one of the main coffee disease. This disease causes the early fall of the leaves and the consequent drought of the productive branches [2, 1]. When the leaves have a small number of rust foliar damages, the injuries may remain in the plant. However when the severity (percentage of the leaf affected by disease) is high, causes its early fall. In plants susceptible to rust, a single foliar damage may cause the leaf fall [1].

The insect *Leucoptera coffeella* (leaf miner) causes reduction in the leaf area and leaf fall with consequent decrease in photosynthesis, resulting in the drop of the production. The larvae of this pest are small that penetrate directly into the leaf mesophyll without touching the outside environment. The damaged regions dry up and the area under attack increases with the development of caterpillars and the various "mines" [3]. There are some studies related to the classification of foliar damages on leaves of plants and also in the calculation of severity. Zhang, et al. [4] proposed an approach to recognition of diseases in cucumber leaf. The method is divided into three main steps: area segmentation to separate leaf damage area using the *k-means* algorithm, extraction of features of the foliar damaged area, and classification using a sparse representation. The great advantage of this approach is the improvement in the recognition performance of diseases and pests. Pahikkala et al. [5] presented a study focused on images of overlapping leaves analyzing color photographs of different cultures. The identification of species was based on different textures of monocotyledons and dicotyledons leaves. An automatic classifier based on the learning algorithm Regularized Least-Squares was used.

Aakif, and Khan [6] proposed an algorithm to identify a plant in three stages: preprocessing, where segmentation is performed with excess green and threshold; in the second stage, extraction of morphological features and application of Fourier descriptors. In the third and last stage, the classification was performed using an artificial neural network. Singh and Misra [7] presented an algorithm for segmentation of images that is used to detect the damaged area in leaves of plants for later classification of the injuries. The segmentation of the image was done using a genetic algorithm. Hitimana and Gwun [8] proposed an automatic method to detect and estimate severity. The image was processed for background removal and the fuzzy c-means algorithm was applied to the channel V of the YUV color space. In this way, the damaged area becomes evident and severity can be estimated by the ratio of pixels of the injured area divided by the total area of the leaf. Patel and Dewangan [9] proposed a mechanism to detect diseases in leaves of plants combining *k-means* and artificial neural networks. The image can be converted to the HSI color space. The *k-means* algorithm can be then applied to determine the region affected by the disease. After identifying the damaged areas, features can be extracted and then used for training and classification. Rastogi, Arora, and Sharma [10] proposed a methodology divided into two parts: the first one involves image preprocessing, feature extraction and training an artificial neural network. The second phase also involves the acquisition of image, preprocessing, feature extraction, *k-means*, estimation of disease severity and calculation of the severity

using fuzzy logic. Prasetyo et al. [11] applied threshold segmentation along with the Otsu method. The method can be applied to the H, S and V channels of the HSV color space and Cb and Cr channels of the YCbCr color space for the mango leaf images. Mwebaze and Owomugisha [12] presented a scale (1 to 5) to calculate disease incidence and severity, where 1 means a totally healthy plant and 5 a plant with maximum severity. Mohanty, Hughes, and Salathé [13] presented another approach for classification of plant diseases using convolutional neural networks. There were 14 species and 26 types of diseases. The results presented an accuracy of 99.35%. So, there are some recent studies for segmentation, feature extraction and classification of plant diseases. The early detection of the disease or pest is fundamental to correct control. In addition, determining the severity of the foliar damaged area may help in decision-making process for the farmer. Garçonet al. [2] shows that a disease control system based on the value of the disease severity is efficient because it saves costs with pulverization. Both tasks recognition and estimation of severity, may be difficult for farmers with little experience. Currently, there are no accessible tools that facilitate these tasks. In most cases, these estimates are made visually or through applications that are not accurate.

In this work, we develop a system for automatically classification of foliar damages of coffee leaves and calculation of its severity. In addition, we show valuable results regarding the image capture process, the background choice, the dataset creation, the best segmentation algorithms, the most suitable neural network for classification and finally the calculation of severity. The system receives as input an image captured by a smartphone, then it identifies the leaf of the coffee tree in the image by means of segmentation, identify the foliar damage contained in the leaf and classify them as well as to calculate the percentage of damaged area. In this case, the damages considered are the coffee leaf rust and coffee leaf miner. It is worth mentioning that there are other diseases and pests not considered in this work [1]. The article is structured as in the following: Section 2 describes algorithms for segmentation, feature extraction and classification of coffee injured leaves and presents an automatic method to calculate the severity. Sections 3 presents the experiments carried out with comparisons and analysis of the results. Section 4 is development of a mobile solution by implementing an App. Section 5 draw conclusions and present directions for future works.

2. Algorithms for Digital Image Processing of Coffee Leaves

The standard steps in digital image processing consists of: 1) segmentation; 2) feature extraction, 3) classification. In some cases the pre-processing is included, which may or not be required depending on the problem.

2.1. Color Space

2.1.1. The color space YCbCr

In the YCbCr color space, the Y component contains only luminance. The components of blue chrominance (B-Y) abbreviated by Cb and red chrominance (R-Y) abbreviated by Cr are not influenced by lumi-

nance [14]. The transformation of RGB to YCbCr is obtained by Equation 1 according [14].

$$\begin{bmatrix} Y \\ Cb \\ Cr \end{bmatrix} = \begin{bmatrix} 16 \\ 128 \\ 128 \end{bmatrix} + \frac{1}{256} \begin{bmatrix} 65.481 & 128.553 & 24.966 \\ -37.797 & -74.203 & 112 \\ 112 & -93.768 & -18.214 \end{bmatrix} \cdot \begin{bmatrix} R \\ G \\ B \end{bmatrix} \quad (1)$$

where R , G and B are the values of the red, green and blue components, respectively, which typically range from 0 to 255. Since the components of chrominance do not vary with lighting, they are widely used in segmentation.

2.1.2. The color space YCgCr

Very similar to YCbCr, the YCgCr color space also has chrominance components, but differs from YCbCr by replacing the chrominance component of blue with that of green (G-Y) abbreviated by Cg [15]. The transformation of RGB to YCgCr is obtained by Equation 2 according [15].

$$\begin{bmatrix} Y \\ Cg \\ Cr \end{bmatrix} = \begin{bmatrix} 16 \\ 128 \\ 128 \end{bmatrix} + \frac{1}{256} \begin{bmatrix} 65.481 & 128.553 & 24.966 \\ -81.085 & 112 & -30.915 \\ 112 & -93.768 & -18.214 \end{bmatrix} \cdot \begin{bmatrix} R \\ G \\ B \end{bmatrix} \quad (2)$$

where R , G and B are the values of the red, green and blue components, respectively, which typically range from 0 to 255. Since the components of chrominance do not vary with lighting, they are widely used in segmentations.

2.1.3. The color space HSV

The HSV color space represents the colors in terms of matrix or color depth (Hue), abbreviated by H, color purity (Saturation), abbreviated by S, and intensity of the value or brightness of the color (Value), abbreviated by V. The components of the HSV color space is obtained by Equations 3, 4 and 5 according [16].

$$H = \arccos \frac{\frac{1}{2}(2R - G - B)}{\sqrt{(R - G)^2 - (R - B)(G - B)}} \quad (3)$$

$$S = \frac{\max(R, G, B) - \min(R, G, B)}{\max(R, G, B)} \quad (4)$$

$$V = \max(R, G, B) \quad (5)$$

where R , G and B are the values of the red, green and blue components respectively, which typically range from 0 to 255.

2.2. Segmentation

The process of segmentation may be thought of as the process of grouping an image in homogeneous units with respect to one or more features [16]. The segmentation of colored images is divided into four groups: edge detection methods; neighborhood-based methods; methods based on histogram; and clustering-based segmentation [17].

2.2.1. Otsu Method

Segmentation of images based on histograms consists mainly in determining a threshold value. Due to the gray levels that characterize the objects in a grayscale image, it is sought to highlight background objects based on one-dimensional statistics, e.g., histograms of gray levels. Ideally, algorithms do this automatically by selecting the best threshold to determine what is background and what is not (object of interest) of an image [18, 19].

The Otsu method [20] selects a global optimal threshold by maximizing the variance between classes. In a two-level thresholding, the pixel that has a gray level lower than the threshold will be assigned to the background, otherwise it will be considered as an object part [18].

Assuming that a two-dimensional image is represented in L gray levels $[0, 1, \dots, L - 1]$, the number of pixels at level i is denoted by n_i , and the total number of pixels is denoted by $N = n_1 + n_2 + \dots + n_L$. Given this distribution, the probability of a gray level is given by Equation 6 according [19].

$$p_i = n_i/N, \quad p_i \geq 0, \quad \sum_{i=0}^{L-1} p_i = 1 \quad (6)$$

In a two-class thresholding, the pixels of the image are divided into classes C_1 with the gray levels $[0, 1, \dots, t]$, and C_2 with the levels $[t + 1, \dots, L - 1]$ by the threshold t . The probability distributions from the grayscale to the two classes were given by Equations 7 and 8 according [19].

$$w_1 = \Pr(C_1) = \sum_{i=0}^t p_i \quad (7)$$

$$w_2 = \Pr(C_2) = \sum_{i=t+1}^{L-1} p_i \quad (8)$$

which is the sum of the probabilities of the gray levels of each one of the classes. The mean of classes C_1 and C_2 were respectively, given by Equations 9 and 10 according [19].

$$u_1 = \sum_{i=0}^t ip_i/w_1 \quad (9)$$

$$u_2 = \sum_{i=t+1}^{L-1} ip_i/w_2 \quad (10)$$

The total mean of the gray levels, represented by u_t is calculated by Equation 11 according [19].

$$u_T = W_1 u_1 + W_2 u_2 \quad (11)$$

The variances of C_1 and C_2 were, respectively calculated by Equations 12 and 13 according [19].

$$\sigma_1^2 = \sum_{i=0}^t (i - u_1)^2 p_i / W_1 \quad (12)$$

$$\sigma_2^2 = \sum_{i=0}^t (i - u_1)^2 p_i / W_2 \quad (13)$$

The interclass variance and variance between classes were respectively, calculated by Equations 14 and 15 according [19].

$$\sigma_w^2 = \sum_{k=1}^2 W_k \sigma_k^2 \quad (14)$$

$$\sigma_B^2 = W_1 (u_1 - u_T)^2 + W_2 (u_2 - u_T)^2 \quad (15)$$

The Otsu method [19] chooses the best threshold t by maximizing variance between classes, which is equivalent to minimizing interclass variance. The threshold value t were calculated by Equations 16 and 17 according [19].

$$t = \arg\{\max_{0 \leq t \leq L-1} \{\sigma_B^2(t)\}\} \quad (16)$$

$$t = \arg\{\min_{0 \leq t \leq L-1} \{\sigma_W^2(t)\}\} \quad (17)$$

The goal is then to iterate through all possible values for the threshold in an image, seeking the one that maximizes the variance between classes. The pseudocode of the Otsu method is described in Algorithm 1.

Algorithm 1 Otsu Method

Require: Image in L grey level;

```
1:  $t \leftarrow 0$ ;
2:  $t_{max} \leftarrow -1$ ;
3:  $variance_{max} \leftarrow -1$ ;
4: for each gray level  $t$  in  $[1, 2, \dots, L - 1]$  do
5:    $W_1 \leftarrow Pr(C_1)$  according to Equation 7;
6:    $W_2 \leftarrow Pr(C_2)$  according to Equation 8;
7:   Compute mean of classes  $C_1$  and  $C_2$  according to Equation 9 and 10;
8:    $v \leftarrow \sigma_B^2$ 
9:   if  $v > variance_{max}$  then
10:      $variance_{max} \leftarrow v$ ;
11:      $t_{max} \leftarrow t$ ;
12:   end if
13: end for
14: for each pixel  $p$  in the image do
15:   if  $p \geq t_{max}$  then
16:     Define pixel  $p$  as white;
17:   end if
18:   if  $p < t_{max}$  then
19:     Define pixel  $p$  as black;
20:   end if
21: end for
22: return Binary image;
```

2.2.2. k -means algorithm

k -means clustering was a method proposed by Macqueen [21] that was commonly used to partition a set of data into k groups [22, 19].

The algorithm consists in initially selecting k centers of random groups (centroids) in a data set (instances) and iteratively refine them. For each instance of the dataset, one calculates the Euclidean distance of this data for each of the centroids by:

$$dist(\mathbf{d}, \mathbf{c}) = \sqrt{\sum_{i=1}^n (d_i - c_i)^2} \quad (18)$$

where $\mathbf{d} = (d_1, d_2, \dots, d_n)$ and $\mathbf{c} = (c_1, c_2, \dots, c_n)$ are two points in n -dimensional Euclidean space. At each new iteration, the centroid of each group is recalculated and the distances are recalculated again. The algorithm converges when there are no significant changes in the centroids.

For the calculation of each centroid c_i of each group $i \in [1, 2, \dots, k]$ is used the mean as described by:

$$c_i = \frac{\sum_{j=1}^n d_j}{n} \quad (19)$$

where n is the number of data in a given group.

In digital image processing, the input set is all pixels of the image. The distance is calculated with the numerical values of each pixel, i.e., the *k-means* group pixels with similar colors in the same group, thus separating objects belonging to the image.

2.2.3. Segmentation on the color space YCgCr

Feng and He [23] proposed a threshold-based segmentation method for foliar damages in leaves of plants. The goal is to highlight the injured leaf to extract features of the foliar damages. The method applies iterative threshold segmentation in the color space YCgCr [15].

The segmentation method initially calculates the difference matrix of Cr and Cg components according to:

$$im_{dif}(x, y) = Cr(x, y) - Cg(x, y) \quad (20)$$

where im_{dif} represents the difference between the pixels of the Cr component at the (x, y) position and the Cg component at the (x, y) position. The pixels are then separated into two groups, one being the damaged foliar area and the other not, according to the threshold. At each new iteration, the threshold is calculated based on the mean of the two groups and the global mean.

According to [23] the algorithm works well for segmentation of foliar damages with brown, red and yellow tones. Algorithm 2 presents the pseudocode of iterative thresholding segmentation.

Algorithm 2 Segmentation on the color space YCgCr

Require: Cg and Cr channels with dimensions $m \times n$;

- 1: Initializes $T \leftarrow 0$;
 - 2: **repeat**
 - 3: Divides the im_{dif} matrix using T into two groups;
 - 4: $G_1 \leftarrow im_{dif} > T$;
 - 5: $G_2 \leftarrow im_{dif} \leq T$;
 - 6: $m_1 = \frac{\sum_{i=0}^{m-1} \sum_{n=0}^{n-1} G_1(m,n)}{m \times n}$;
 - 7: $m_2 = \frac{\sum_{i=0}^{m-1} \sum_{n=0}^{n-1} G_2(m,n)}{m \times n}$;
 - 8: The new threshold:
 - 9: $T \leftarrow (m_1 + m_2)/2$;
 - 10: **until** Convergence;
 - 11: **return** Matrix G_1 and G_2 ;
-

2.3. Feature extraction

In order to obtain good results in the subsequent stages of processing, it is necessary to create a set of attributes that will be used in the training stage, and later in the classification phase [24]. It is important to note that, in this step, the input is still an image but the output is a set of measures corresponding to that image.

Extracting features (attributes) from an image highlights differences and similarities between objects. Among these features, one can include the brightness of a region, the texture, the amplitude of the histogram, among others. In general, the extraction of features is a process usually associated to the analysis of the regions of an image [25].

2.3.1. Texture Attributes

Texture contain important information about the structural arrangement of surfaces and their relationships with the medium [26]. It is possible to obtain the texture attributes by means of the Gray Level Co-occurrence Matrix (GLCM) that was initially described by Harlick et al. [26]. This methodology explores the dependence of the gray levels of the texture to assemble the GLCM. This matrix represents the relative frequency with which neighboring pixels occur in the gray-scale image [24, 26].

Next, some texture attributes that are measured from the co-occurrence matrix [26] are presented. In the following equations, L represents the gray levels that compose the image, $p(i, j)$ represents the relative frequency with which neighboring pixels occur in the image, i and j the gray levels in the GLCM.

1. **Energy or second angular momentum:** Measures the textural uniformity. High values of this

attribute indicate that the distribution of the gray level in the image has a uniform distribution [27].

$$Energy = \sum_{i,j=0}^{L-1} p(i,j)^2 \quad (21)$$

2. **Contrast:** It is the difference between the highest and lowest values of gray of a set of adjacent pixels [27].

$$Contrast = \sum_{i,j=0}^{L-1} p(i,j)(i-j)^2 \quad (22)$$

3. **Homogeneity:** Measures the homogeneity of an image. This attribute assumes higher (larger) values when there only small differences in tones (shades) of gray in the pixel sets. Therefore, homogeneity and contrast are inversely correlated [27].

$$Homogeneity = \sum_{i,j=0}^{L-1} \frac{p(i,j)}{1 + (i-j)^2} \quad (23)$$

4. **Dissimilarity:** This measure increases linearly as it moves away from the diagonal, unlike contrast, which increases exponentially.

$$Dissimilarity = \sum_{i,j=0}^{L-1} p(i,j)|i-j| \quad (24)$$

5. **Correlation:** It is a measure of linear dependence on the image. High correlation values imply a linear relationship between the gray levels of neighboring pixels [27]

$$Correlation = \sum_{i,j=0}^{L-1} \frac{ijp(i,j) - \mu_x\mu_y}{\sigma_x\sigma_y} \quad (25)$$

where,

$$\mu_x = \sum_i^{L-1} ip(i,*) \quad (26)$$

$$\mu_y = \sum_j^{L-1} ip(*,j) \quad (27)$$

$$\sigma_x = \sqrt{\sum_i^{L-1} (i - \mu_x)^2 p(i,*)} \quad (28)$$

$$\sigma_y = \sqrt{\sum_j^{L-1} (j - \mu_y)^2 p(*,j)} \quad (29)$$

$$p(i,*) = \sum_j^{L-1} p(i,j) \quad (30)$$

$$p(*,j) = \sum_i^{L-1} p(i,j) \quad (31)$$

Other variables used to quantify textures are based on first order statistics that are calculated in a subregion [27]. These first-order attributes do not take into account the spatial distribution of gray levels in a region of the image. They can be calculated by the frequency distribution of the gray levels of the pixels of an image [24].

Next, $P(i)$ is the relative frequency with which the gray level i occurs in the region, and M is the average of the gray levels of the region [27]. L are all gray levels in the image.

1. **Variance:** It is a measure of statistical dispersion. The higher the variance, the more distant from the mean will be the levels of gray. It is defined by:

$$Variance = \sum_i^{L-1} [i - M]^2 P(i) \quad (32)$$

2. **Kurtosis:** It characterizes the flattening of the curve of the probability distribution function. It is defined by:

$$Kurtosis = \frac{\sum_i^{L-1} (i - M)^4 P(i)}{V^2} \quad (33)$$

where V is the variance.

3. **Entropy:** It measures the clutter of an image. When an image does not have a uniform texture the entropy is high [27]. It is defined by:

$$Entropy = - \sum_i^{L-1} P(i) * \log P(i) \quad (34)$$

2.3.2. Color attributes

The values of mean, standard deviation and variance can be used in color attributes. Next, in the Equations 35 and 36 $I(i, j)$ represents the pixel value of the image at position (i, j) . The input image has dimensions $m \times n$ [28, 29].

1. **Mean:** The mean is the sum of the values of all pixels in the image. It can be applied to each of the RGB channels of the input image. The mean is calculated by:

$$\mu = \frac{\sum_i^{m-1} \sum_j^{n-1} I(i, j)}{m \times n} \quad (35)$$

2. **Deviation:** For each RGB channel of the image, the standard deviation is calculated by:

$$\sigma = \frac{\sum_i^{m-1} \sum_j^{n-1} (I(i, j) - \mu)^2}{m \times n} \quad (36)$$

Methods for extraction of attributes allows a better discrimination of the classes in the classification process. In this work, the attributes are represented by vectors containing values extracted from the images [25].

For this work, the following attributes were selected after an in depth experimental study:

- Distributional attributes: mean, standard deviation, kurtosis and entropy. Each of them is applied to each RGB component of the injured foliar area [29].
- Attributes of co-occurrence: contrast, dissimilarity, homogeneity, energy and correlation. All attributes are calculated from the co-occurrence matrix [7].

2.4. Classification Algorithms

Classification is the process of assigning a label to an object based on its features translated by its descriptors. Data classification is present in several real problems such as: recognizing patterns in images, differentiating species of plants, classifying between benign and malignant tumors, among others [30]. There are several algorithms for classifying data. In this work, Artificial Neural Network (ANN) trained with Backpropagation, and Extreme Learning Machine (ELM) are used.

2.4.1. Artificial Neural Networks

Artificial Neural Networks can be described as a mapping of a input set to an output set [31, 32]. It resembles human brain in two aspects: 1) Knowledge is acquired by the network through a learning process. 2) Interconnections between neurons, known as synaptic weights, are used to store the knowledge acquired. A neuron is a fundamental processing unit for the operation of a neural network. They are simplifications of the biological neuron [33].

The basic elements in a neuron are [32]: a) A set of synapses where each of them has an associated weight. Specifically, a signal x_j at the input of the synapse j connected to neuron k , is multiplied by the synaptic weight w_{kj} . b) An adder, to sum up all the input signals multiplied by the respective synaptic weights. The operations described here constitute a linear combination. c) An activation function to limit the output amplitude of each neuron. Normally, the variation of the output amplitude y_k of neuron k is a closed interval in the range $[0,1]$ or $[-1,1]$.

Figure 1 shows the model of an artificial neuron.

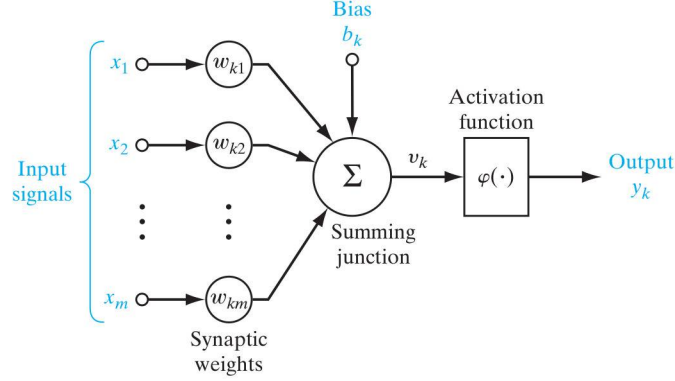


Figure 1: Representation of an artificial neuron.

In the summing junction, the bias (b_k) is also taken into account. Therefore, a neuron k is described by:

$$y_k = \varphi(\mathbf{x}, \mathbf{w}, \mathbf{b}) = \varphi\left(\sum_{j=1}^m w_{kj}x_j + b_k\right) \quad (37)$$

where x_j are the scalar values of the input, m is the size of the input, b_k are the bias, w_k are the weights learned by ANN and $\varphi(\cdot)$ is the activation function of the neuron. The activation function $\varphi(\cdot)$, defines the output of the neuron in terms of v_k . The most frequently used are: the sigmoid, the hyperbolic tangent and Relu [32].

An ANN architecture is related to the way the neurons are connected to each other, how they are grouped in layers and the learning algorithms used in training of the weights. The multi-layer feedforward network has 3 types of layers, where the outputs of a layer are the inputs of the following layer. The architecture is made up of: 1) Input layer, which is the layer connected immediately to the values of the inputs to be processed. 2) Intermediate or hidden layers, the neurons corresponding to these layers are called hidden neurons. The term hidden corresponds to the fact that this part of the network can not be seen directly from the input or output. The addition of hidden layers of neurons enables the extraction of several high-order statistics. These layers are responsible for learning the representation of network information [32]. 3) Output layer: In this layer, the goal is to adjust the internal information of the network in a format suitable for use.

In Figure 2, is shown a Single Feedforward Neural Network (SLFN) with a single hidden layer, 10 input values, 4 neurons in the hidden layer, and 2 neurons in the output layer.

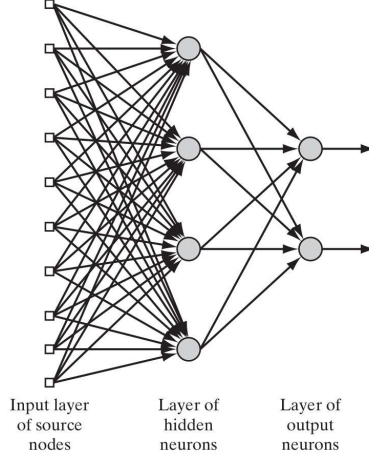


Figure 2: Single Layer Feedforward Neural Network.

Learning in a neural network is a process by which the parameters (synapses \mathbf{w}) of the network are adapted through a process of stimulation by the environment in which the network is inserted. The type of learning is determined by the way in which the modification of the parameters occurs. Two basic learning paradigms are unsupervised and supervised learning [32]. In this work we use two supervised learning algorithms for training the SLFN: 1) Backpropagation and 2) Extreme Learning Machines (ELM).

2.4.2. Backpropagation algorithm

When using supervised learning, it is necessary to minimize a cost function that computes the error between the expected output and the result obtained by the network output. Widely used is the mean square error, which is described by:

$$E(\mathbf{x}, \mathbf{w}, \hat{\mathbf{y}}) = \frac{1}{m} \sum_{k=0}^m (\hat{\mathbf{y}}^{(k)} - \varphi(\mathbf{x}^{(k)}, \mathbf{w}))^2 \quad (38)$$

The Gradient descent is described by:

$$\mathbf{w} = \mathbf{w} - \alpha \frac{\partial E(\mathbf{x}, \mathbf{w}, \hat{\mathbf{y}})}{\partial \mathbf{w}} \quad (39)$$

The backpropagation is the algorithm most used to minimize this function. So, the error is moved down successively towards a minimum point of the error surface; whereas the minimum point may be a local or a global minimum [32].

In Equation 39 the variable α corresponds to the learning rate. The pseudo-code for the network training is described in Algorithm 3.

Algorithm 3 Neural Network Training with Gradient Descent

Require: Training data set $(\mathbf{x}, \hat{\mathbf{y}})$; Learning rate α ;

- 1: $\mathbf{w} \leftarrow$ random initialization of the weights according to a uniform distribution in range $[-1, 1]$;
 - 2: **repeat**
 - 3: $a \leftarrow X$;
 - 4: **for each** layer $[1, 2, \dots, |\mathbf{w}|]$ **do**
 - 5: $a \leftarrow f(a, w_i)$ according to Equation 37;
 - 6: **end for**
 - 7: Update weights according to Equation 39;
 - 8: **until** Convergence;
 - 9: **return** Matrix G_1 and G_2 .
-

2.4.3. Extreme Learning Machine

Essentially, extreme learning machine was originally developed for SLFN. ELM aims to find not only the smallest training error but also the lower norm of the output weights [34].

The weights of the input layer neurons and bias are initialized with random values, and the weights of the neurons of the output layer are calculated analytically without using iterative processes. The mathematical formulation of ELM is described by [35, 36] through the following equation:

$$\sum_{i=1}^{\tilde{N}} \beta_i g(\mathbf{w}_i \cdot \mathbf{x}_j + b_i) = \mathbf{t}_j, \quad j = 1, \dots, N \quad (40)$$

where,

- \tilde{N} is the number of hidden neurons and N is the number of training samples.
- $\mathbf{x}_j = [x_{j1}, x_{j2}, \dots, x_{jn}]^T$ is the j -th input vector and represents each different samples.
- $\mathbf{t}_j = [t_{j1}, t_{j2}, \dots, t_{jm}]^T$ is the j -th output target vector and represents the expected outputs with respect to a sample input vector \mathbf{x}_j .
- $\mathbf{w}_i = [w_{i1}, w_{i2}, \dots, w_{in}]^T$ represents the vector of weights that connects the i -th neuron of the hidden layer to the neurons of the input layer.
- $\beta_i = [\beta_{i1}, \beta_{i2}, \dots, \beta_{im}]^T$ represents the vector of weights that connects the i -th neuron of the hidden layer to the neurons of the output layer.
- b_i represents the bias associated to the i -th neuron of the hidden layer.
- $g(\cdot)$ is the activation function.

The N equations presented above are described in simplified form by $\mathbf{H}\hat{\boldsymbol{\beta}} = \mathbf{T}$, whose matrix form is given by:

$$\mathbf{H} = \begin{bmatrix} g(\mathbf{w}_1 \cdot \mathbf{x}_1 + b_1) & \dots & g(\mathbf{w}_{\tilde{N}} \cdot \mathbf{x}_1 + b_{\tilde{N}}) \\ \vdots & \ddots & \vdots \\ g(\mathbf{w}_1 \cdot \mathbf{x}_N + b_1) & \dots & g(\mathbf{w}_{\tilde{N}} \cdot \mathbf{x}_N + b_{\tilde{N}}) \end{bmatrix}_{N \times \tilde{N}} \quad \hat{\boldsymbol{\beta}} = \begin{bmatrix} \beta_1^T \\ \vdots \\ \beta_{\tilde{N}}^T \end{bmatrix}_{\tilde{N} \times m} \quad \mathbf{T} = \begin{bmatrix} \mathbf{t}_1^T \\ \vdots \\ \mathbf{t}_N^T \end{bmatrix}_{N \times m} \quad (41)$$

The determination of the output weights, which connect the neurons of the hidden layer to the output layer is defined as the Least-Squares solution of the linear system $\mathbf{H}\hat{\boldsymbol{\beta}} = \mathbf{T}$, which is given by $\hat{\boldsymbol{\beta}} = \mathbf{H}^\dagger \mathbf{T}$, where \mathbf{H}^\dagger is the generalized inverse of Moore-Penrose's matrix \mathbf{H} [35, 36]. The pseudo-code of the ELM training is presented in Algorithm 4.

Algorithm 4 ELM training

Require: Training data set $(\mathbf{x}, \hat{\mathbf{y}})$; Learning rate α ;

- 1: Preprocessing of the input samples;
 - 2: Initialization of weights and bias between the first and hidden layer with random values;
 - 3: Set the number of neurons in the hidden layer;
 - 4: Calculation of the matrix H according to Equation 41;
 - 5: Calculation of $\hat{\boldsymbol{\beta}}$ according to $\hat{\boldsymbol{\beta}} = \mathbf{H}^\dagger \mathbf{T}$;
 - 6: **return** $\hat{\boldsymbol{\beta}}$.
-

2.5. Severity calculation

Knowing the presence or absence of disease or pest is important for the farmer. However, knowing the severity of the disease is extremely important so that measures can be taken to avoid loss of crop yields. In addition, this measure brings important information over time on the resistance of the disease or pest and its progress [12, 1].

There are some methods for estimating the damaged foliar area. The two most common are: 1) the estimation of the severity by manual calculation of the damaged foliar area in the leaf with the use of measuring tools; 2) estimation visually based on a diagrammatic scale.

In this work, the severity estimation consists of the count of the image pixels belonging to the injured area of the leaf. One calculates the severity according to

$$Severity = \frac{A_{damaged}}{A_{leaf}} \times 100 \quad (42)$$

where, $A_{damaged}$ is the area of the injured region of the leaf image in pixels, and the A_{leaf} is the total area of the leaf in pixels.

2.6. Proposed Approach

It is expected a system for automatic classification of damaged foliar in coffee leaves and calculation of severity. The system receives as input an image captured by the smartphone, then identify the leaf of the

coffee in the image by means of the segmentation, identify the damaged foliar area contained in the leaf and classify. In addition, it calculates the percentage of injured area as shown in Figure 3. In this study, the damaged foliar area considered in the leaf of the coffee tree was the coffee leaf miner and the coffee leaf rust, although there were other diseases and pests not considered in this work [1].

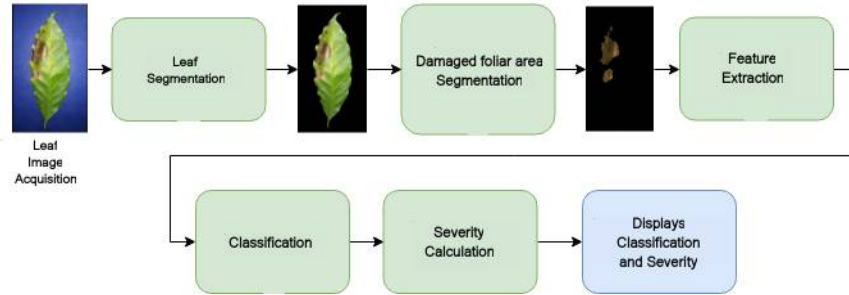


Figure 3: Overview of the automatic process for classification of the damaged foliar area and calculation of the degree of severity of the coffee leaf from images obtained with smartphone.

3. Experimental results

3.1. Database

The images used in this work were captured using the ASUS Zenfone 2 smartphone (ZE551ML) with a resolution of 10 Megapixels (4096x2304 pixels). Three background colors were used: white; black and blue. Table 1 shows the amount of images contained in the dataset. The database consists of 690 images, divided according to Table 1. They are available from authors upon request.

Class	White background	Blue background	Black background	Total number
Normal	58	58	58	174
Leaf miner	88	88	88	264
Rust	84	84	84	252

Table 1: Dataset division.

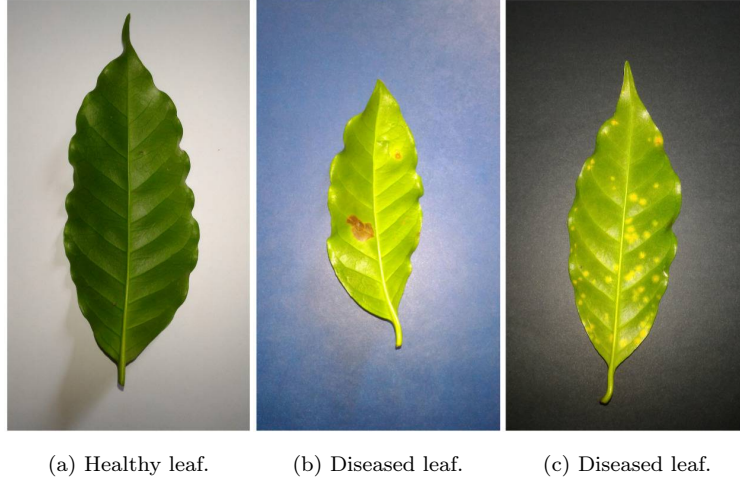


Figure 4: Images of coffee leaf submitted to the segmentation process.

The leaves containing coffee leaf miner and coffee leaf rust were segmented from 230 images with white background and divided into two classes according to Table 2.

Class	Number of images
Coffee leaf miner	256
Coffee leaf Rust	759

Table 2: Imbalanced dataset.

For training of the classification algorithms is used the balanced dataset as shown in Table 3. The class imbalance problem in training of the classifier usually does affect performance, especially for small and moderate training data sets that contain correlated or uncorrelated features [37].

Class	Number of images
Coffee leaf miner	256
Coffee leaf rust	256

Table 3: Balanced dataset.

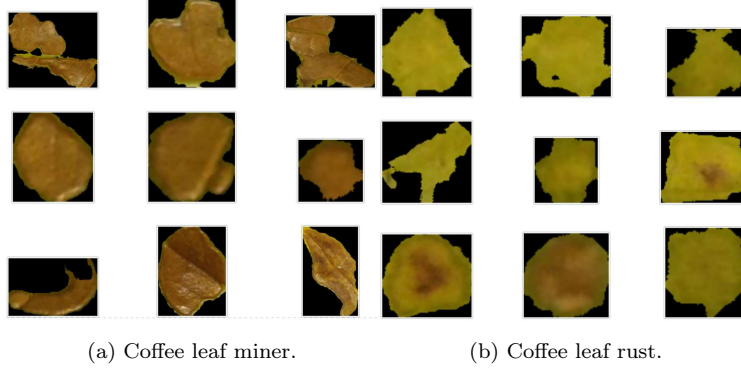


Figure 5: Foliar damages

3.2. Evaluation of the Segmentation Results

The metric used to evaluate the segmentation algorithms is the same as used in [23] and [38]. The metric is defined by the Recognition Working Group (Automatic Target Recognition Working Group (ATRWG)). The segmentation precision is defined by:

$$Q_{seg} = \frac{\sum_{k,j=0}^{k,j=m,n} (A(i)_{k,j} \cap B(i)_{k,j})}{\sum_{k,j=0}^{k,j=m,n} (A(i)_{k,j} \cup B(i)_{k,j})} \quad (43)$$

where A is the segmentation of the algorithm under evaluation, B is the manual segmentation that should be optimal. The index $i = 255$ indicates the pixels that are considered as leaf and $i = 0$ are the pixels considered as background. k and j are the row and column indices respectively of the pixel in the image, where the total number of rows is m and columns is n .

According to Equation 43, the leaf segmentation is based on the logical operations " \cap " and " \cup ", comparing pixel to pixel of the resulting mask A with the ideal mask B . The Q_{seg} measure varies between 0 and 1, where, $Q_{seg} = 1$ indicates that the segmentation is perfect and $Q_{seg} = 0$ indicates that the segmentation is not correct.

3.2.1. Leaf Segmentation

To ensure quality in the feature extraction, especially in the calculation of the severity, which depends directly on the area of the leaf, it is necessary that the segmentation process works correctly. So, for a good result in the segmentation, the following procedures are adopted [11]:

1. Transform the input image into the HSV or YCbCr color space.
2. Select the best component.
3. Apply the Otsu method [20] to obtain the threshold for segmentation.
4. Apply the threshold to get the binary image.

5. Apply the morphological operations of opening and closing for elimination of noise and filling of failures in the binary image.

To determine the best component for application of the Otsu method, it is necessary to evaluate each binary mask resulting from the segmentation in each channel. Segmentation quality is evaluated based on the metric described by Equation 43. For purpose of comparison, 20 leaf images in the three different backgrounds (white, black and blue) were chosen in order to find out the best background to be used in the segmentation process. The masks manually segmented were obtained using Photoshop as shown in Figure 6.

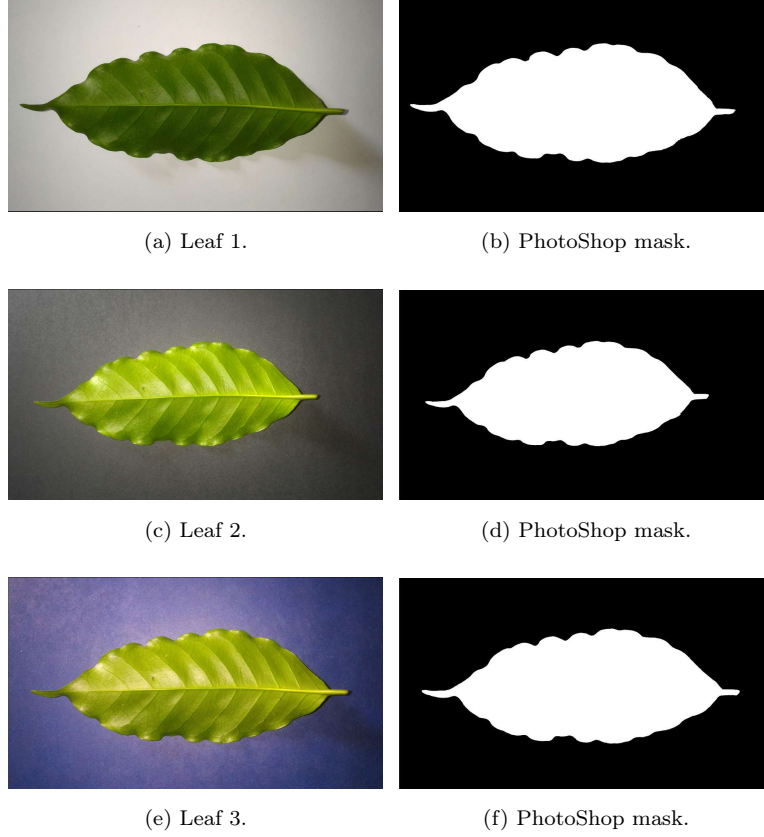


Figure 6: Masks using PhotoShop.

The results for segmentation accuracy are listed in Table 4.

Background	Qseg					
	CbS	Cb	Cr	H	S	V
White	0,978	0,961	0,680	0,746	0,990	0,845
Blue	0,828	0,970	0,729	0,770	0,755	0,018
Black	0,983	0,972	0,222	0,265	0,982	0,722

Table 4: Accuracy of segmentation for different backgrounds and color components.

The segmentation quality depends on the background used and the color component. For example, by using the blue background, it is not recommended to use the component V but rather the component Cb. The CbS component in Table 4 is a mixture of the Cb and S component aiming at a better segmentation. In this case, for the black background this approach was more effective. The images of the leaf segmentation process are shown in Figure 7.

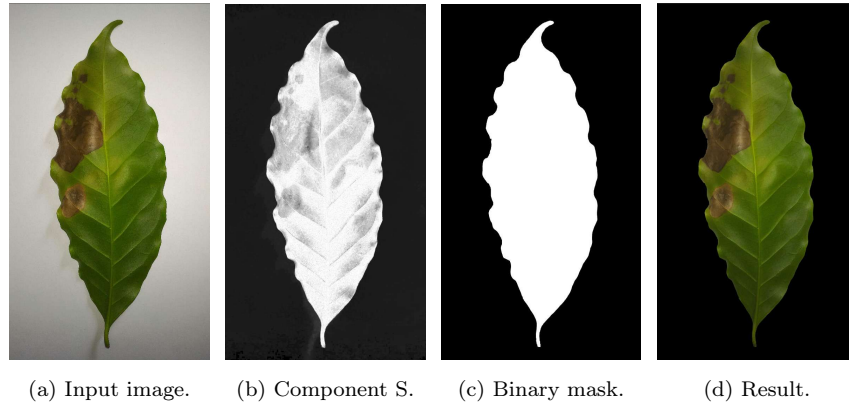


Figure 7: Images of the leaf segmentation process.

The high accuracy of the images segmentation using white background in the S component of the HSV color space is evident by analysing the histogram of this component as shown in Figure 8. This shows that the use of the Otsu method works pretty well, since the histogram is bimodal. Therefore, determining a threshold for the separation between leaf and background was in this case quite easy.

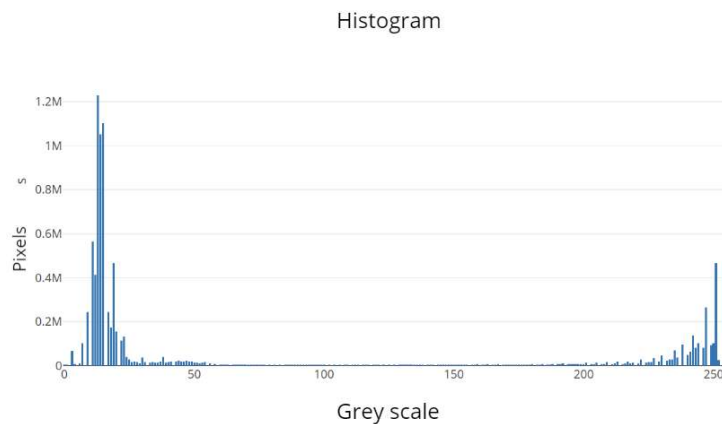


Figure 8: Histogram for the S component in HSV color space.

3.2.2. Segmentation of injured coffee leaves

After the process of segmentation of the leaf it is necessary to segment of injured coffee leaves. This step is also very important because it directly influence the quality of the attributes that are extracted from the damaged area and in the calculation of severity. The segmentation process of injured coffee leaves can be

listed as follows:

1. Transform the input image of the leaf already segmented into the HSV and YCgCr color space, where the components are shown in Figure 9.
2. Apply iterative threshold segmentation algorithm in the YCgCr color space [15], or apply segmentation using the *k-means* algorithm in component Cr.

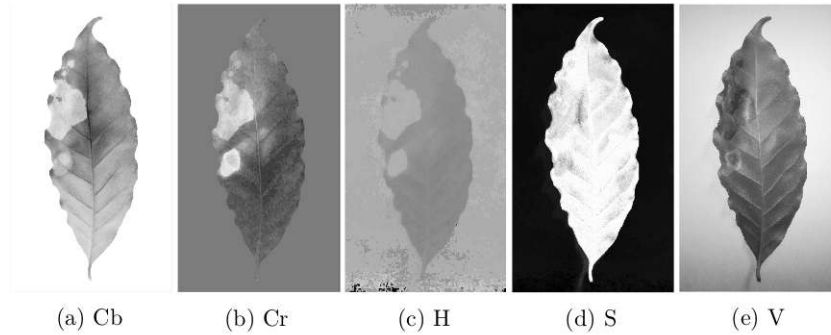


Figure 9: Components of the color space YCbCr and HSV.

For the segmentation of the foliar damages two algorithms are compared: the *k-means* algorithm applied to the Cr component of the image converted to the YCbCr color space; or the iterative threshold segmentation method applied in the converted image to the YCgCr color space [15]. For the iterative threshold algorithm [15], the stopping criterion is reached when the difference between thresholds of 600 successive iterations is less than or equal to 0.0001. For the *k-means* algorithm, the input parameter is the number of random centroids. In our case, $k = 3$ was used. For values of k lower than this, the injured leaf area end up not being properly separated of the rest of the image.

In Figure 10 is shown the target mask manually obtained through Photoshop and the other tested.

The results of segmentation of damaged foliar area for each method are presented in Table 5.

	White background		Blue background		Black background	
Evaluation	k-means	YCgCr	k-means	YCgCr	k-means	YCgCr
Qseg	0,975	0,976	0,949	0,879	0,487	0,924
Time (s)	15,21	6,32	16,52	7,10	14,43	6,52

Table 5: Comparison between k-means algorithm and YCgCr for different backgrounds.

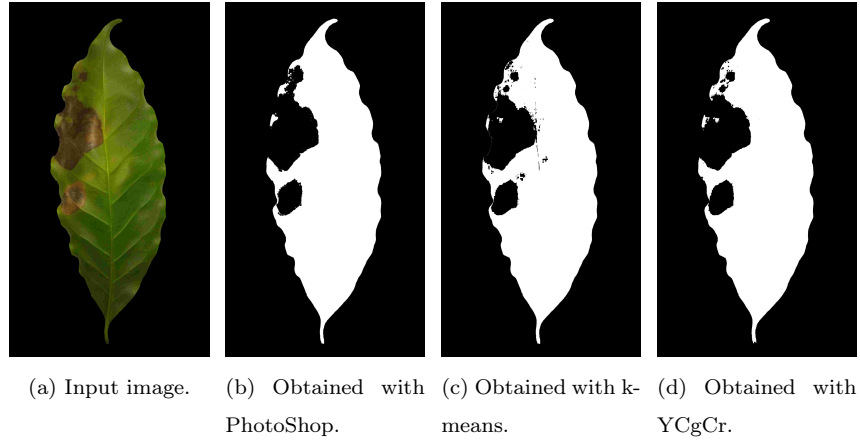


Figure 10: Masks generated from the segmented leaves.

It can be observed that the method using iterative threshold in YCgCr color space is more accurate in the segmentation and also faster than the *k-means*. The white background also shows better results for injured leaf separation. This was mainly because the camera, at the time of capture, was in the automatic color adjustment mode. Therefore, the different backgrounds generate different color tones in the coffee leaf. In addition, the incidence of flash creates reflective focus on the leaf. Figure 11 shows one of these segmentation errors caused by these anomalies, where the segmentation method encounters damaged foliar areas that did not exist. On the other hand, in Figure 12, is illustrated a case where the segmentation occurred perfectly.

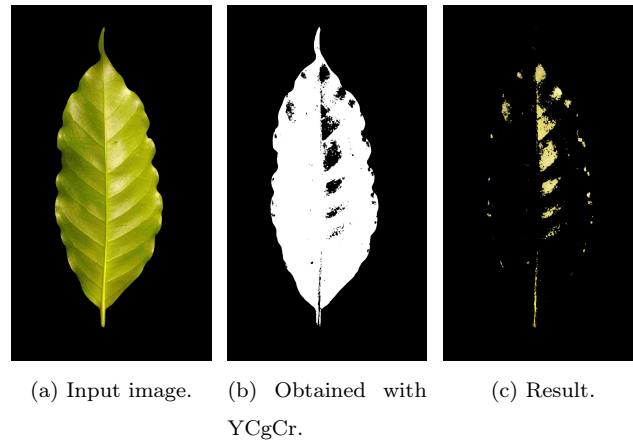


Figure 11: A case showing the occurrence of error in the process of injured leaf segmentation.

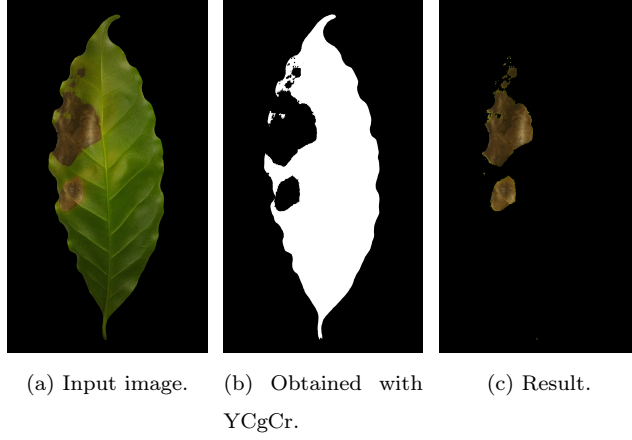


Figure 12: A successful case in the process of injured leaf segmentation.

By mean of these investigations, one can conclude that the best background would be white, since it presents better results to the leaf segmentation as well as to the segmentation of the leaf injured foliar area.

3.3. Classification results

In this work, artificial neural network trained with Backpropagation algorithms and extreme learning machine was used. In both cases the best architecture were evaluated according to the most used metrics: sensitivity and precision [39].

3.3.1. Metrics used

- **Recall:** Denotes the proportion of true positives over the true positives and false negatives described as:

$$Recall = \frac{tp}{tp + fn} \quad (44)$$

where tp is the number of true positives and fn is the amount of false negatives.

- **Precision:** Denotes the proportion of true positives over all positive inferences and described as:

$$Precision = \frac{tp}{tp + fp} \quad (45)$$

where tp is the number of true positives and fp of false positives.

- **Accuracy:** Denotes the proportion of true results (both true positives and true negatives) over the total number of cases examined described as:

$$Accuracy = \frac{tp + tn}{total} \quad (46)$$

where tp is the number of true positives, tn is the amount of true negatives and $total$ is the number of cases examined.

3.3.2. Classification results using Backpropagation

In the neural network training the following setup and parameters were used: Stochastic gradient descent (sgd) was used to minimize the error [40]. Activation function: ReLu was used as it is the most frequently used due to rapid learning [41]. The learning rate tested was 0.001, 0.01; 0.1; 0.2 and 0.3. The stop criterion: the training is interrupted when the difference between the error of two successive iterations is less than 0.0001. Decay: Determines the decay learning rate along the training period. We use a constant decay as well as exponential decay over time. The number of neurons used in the hidden layer started with 10 neurons.

For each configuration, the training was performed 100 times. To each new training, testing and training sets were random chosen, with 70% of data for training and 30% for testing. Table 6 shows the configurations that obtained the best results.

	Parameters				Results	
Model	Neurons in the hidden layer	Learning rate	Update of the learning rate	Accuracy (%)	Precision (%)	Recall (%)
1	20	0.1	Constant	95.527 \pm 0.945	95.906 \pm 0.949	93.428 \pm 0.924
2	30	0.1	Constant	95.824 \pm 0.948	95.959 \pm 0.949	93.142 \pm 0.922
3	40	0.1	Constant	96.013 \pm 0.950	96.151 \pm 0.951	93.233 \pm 0.922
4	50	0.1	Constant	95.726 \pm 0.947	95.970 \pm 0.950	92.688 \pm 0.918
5	100	0.1	Constant	95.815 \pm 0.948	96.191 \pm 0.952	93.181 \pm 0.922
6	200	0.1	Constant	95.958 \pm 0.950	96.053 \pm 0.950	92.766 \pm 0.918
7	10	0.2	Constant	95.175 \pm 0.942	95.277 \pm 0.943	92.363 \pm 0.914
8	20	0.2	Constant	95.041 \pm 0.940	95.501 \pm 0.945	92.857 \pm 0.920
9	30	0.2	Constant	95.027 \pm 0.940	95.526 \pm 0.945	93.103 \pm 0.922
10	40	0.2	Constant	95.212 \pm 0.942	95.098 \pm 0.941	92.311 \pm 0.914
11	50	0.2	Constant	95.307 \pm 0.943	94.728 \pm 0.937	93.000 \pm 0.920
12	100	0.2	Constant	95.136 \pm 0.941	94.882 \pm 0.939	93.155 \pm 0.921
13	200	0.2	Constant	95.220 \pm 0.942	95.324 \pm 0.943	93.025 \pm 0.920

Table 6: Comparison of neural network models with different setup and parameters.

One notices that the best models for this training set are those that use the constant learning rate for values between 0.1 and 0.2 with the number of neurons varying from 10 to 100.

3.3.3. Classification results with extreme learning machine

For training with ELM, the setup and parameters used were Activation function: Linear, sigmoid and hyperbolic tangent functions. The number of neurons 10, 20, 30, 40, 50, 100 and 200 were tested in the

hidden layer. The number of runs for each configuration and the database were the same as described in previous case. Table 7 shows the results of the runs for each configuration.

Models	Parameters		Results		
	Neurons in the hidden layer	Activation func.	Accuracy (%)	Precision (%)	Recall (%)
1	10	Linear	95.815 \pm 0.013	98.160 \pm 0.199	97.350 \pm 0.507
2	20	Linear	96.363 \pm 0.012	98.099 \pm 0.311	97.519 \pm 0.312
3	30	Linear	96.351 \pm 0.028	98.592 \pm 0.090	97.103 \pm 0.247
4	40	Linear	96.386 \pm 0.024	98.363 \pm 0.100	97.460 \pm 0.182
5	50	Linear	96.320 \pm 0.038	98.390 \pm 0.193	97.337 \pm 0.052
6	100	Linear	96.348 \pm 0.013	98.590 \pm 0.153	97.142 \pm 0.455
7	200	Linear	96.357 \pm 0.036	98.644 \pm 0.226	97.649 \pm 0.325
8	10	Sigmoid	92.523 \pm 0.255	94.795 \pm 0.634	87.324 \pm 0.442
9	20	Sigmoid	95.504 \pm 0.120	97.364 \pm 0.322	94.480 \pm 0.065
10	30	Sigmoid	96.958 \pm 0.062	97.802 \pm 0.475	96.207 \pm 0.468
11	40	Sigmoid	97.258 \pm 0.042	97.710 \pm 0.027	97.129 \pm 0.260
12	50	Sigmoid	97.298 \pm 0.035	97.554 \pm 0.298	97.493 \pm 0.078
13	100	Sigmoid	98.128 \pm 0.045	96.442 \pm 0.277	96.701 \pm 0.363
14	200	Sigmoid	99.095 \pm 0.007	93.816 \pm 0.427	92.818 \pm 0.428
15	10	Tang. Hiper.	91.458 \pm 0.226	93.619 \pm 0.110	86.818 \pm 0.377
16	20	Tang. Hiper.	94.440 \pm 0.043	95.349 \pm 0.379	91.909 \pm 0.013
17	30	Tang. Hiper.	95.759 \pm 0.006	96.397 \pm 0.046	94.181 \pm 0.039
18	40	Tang. Hiper.	96.472 \pm 0.075	96.528 \pm 0.062	95.519 \pm 0.182
19	50	Tang. Hiper.	96.965 \pm 0.037	97.075 \pm 0.254	95.740 \pm 0.792
20	100	Tang. Hiper.	97.988 \pm 0.987	96.871 \pm 0.077	96.272 \pm 0.351
21	200	Tang. Hiper.	99.062 \pm 0.003	93.404 \pm 0.536	92.675 \pm 0.584

Table 7: Comparison between ELM models.

The models that use the linear activation function presented, in general, better results for this base. However, we can observe that from 10 to 200 neurons in the models 1-7 the performance improvement was not significant. Another interesting point was the confirmation that the accuracy is not sufficient to evaluate the performance of the classifier, since the model 14 presents a very high accuracy but with lowest values of precision and sensitivity compared to other models. This is probably because the network becomes very specialized for the training set.

Since ELM presents better results when compared to backpropagation, it was used as a classifier for the damaged foliar area classification and severity calculation.

3.4. Severity calculation results

Some works such as in [12], [10] and [42] presented the calculation of severity but do not use metrics to validate the result. Therefore, we calculated the severity of the manually generated masks with the

PhotoShop and compare it with the severity calculation presented in this work. The results of the severity calculation for each one of the methods are presented in Table 8.

	Severity (%)		
Image	k-means	YCgCr	PhotoShop
1	15,05	14,29	15,05
2	2,05	1,98	2,17
3	2,98	3,62	2,81
4	6,25	6,97	6,00
5	10,45	3,93	11,15
6	7,87	6,73	9,95
7	0,89	0,91	0,62
8	6,49	6,62	6,18
9	2,80	2,72	2,69
10	1,64	1,67	1,42

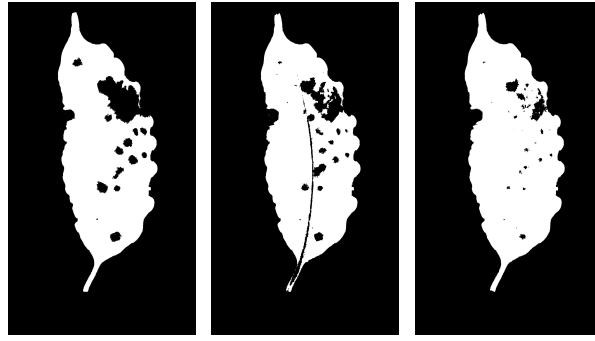
Table 8: Results for severity estimation.

The difference between the severity percentages is acceptable because the assessment of severity is usually done between ranges of values [10], as presented in Table 9. In addition, the segmentation done manually is an approximation of what the author considers as ideal, when in fact, this should be done by a specialist in phytopathology.

Risk	Severity
very low	up to 1%
low	between 1% - 10%
middle	between 10% - 20%
high	between 20% - 40%
very high	between 40% - 100%

Table 9: Risk of severity [10].

For image 5 of Table 8, the result of the severity using the segmentation in YCgCr color space presented great error compared to the other two methods. This is because of the difference between manual segmentation and automatic segmentation in YCgCr. The masks generated by the different methods for this case is deployed in Figure 13.



(a) Input image. (b) Obtained with YCgCr. (c) Result.

Figure 13: Comparison between the injured leaf segmentation masks for the 3 different methods.

In fact, it is clear why the severity calculation is so different. The mask generated by the YCgCr method could not identify the entire damaged foliar area of the leaf. Figures 14 and 15 show the images after the processing with the classification of the injured area and the calculation of severity.



(a) Input image. (b) Segmented. (c) Result.

Figure 14: Pest - Coffee leaf miner; Severity: 3.62%.



(a) Input image. (b) Segmented. (c) Result.

Figure 15: Disease - Coffee leaf rust; Severity: 2.33%.

4. Development of an Application (App)

With the ease of access to the internet and devices such as smartphones, the number of applications that aim to facilitate the tasks for the final users has increased. So, the application developed in this work seeks to integrate the whole process of segmentation of the coffee leaf and its damaged foliar area deploying the results of classification and severity. For the development of the application, the Android system was chosen as it is widely used and has an affordable development platform. The entire image processing step was performed on a server, which receives the image captured by the smartphone, stores it and generates a document with the information to the database, performs the necessary processing by executing the code in Python, saves the information resulting from the processing in the database and sends the results to the application. Full-Stack Mean.js was used for the server development. The platform overview is shown in Figure 16.

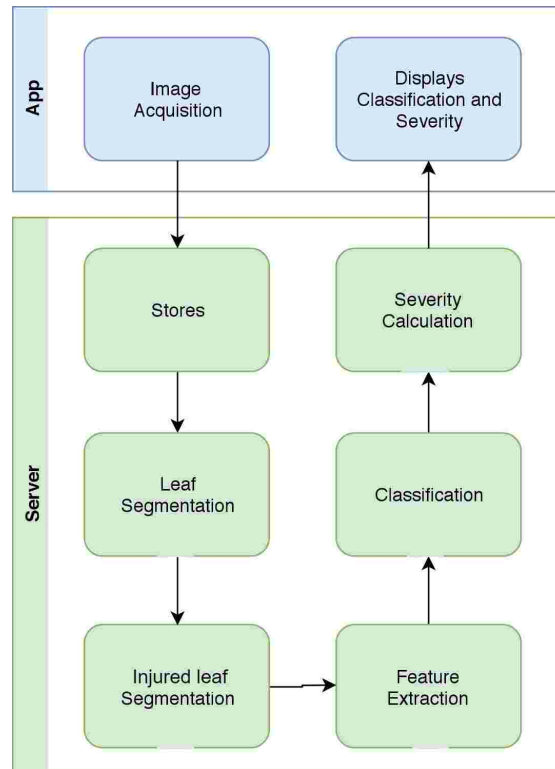


Figure 16: Classification process and severity calculation.

4.1. Used Technologies

4.1.1. Framework Mean.js

The acronym was first used in 2013 by Karpov's development team of MongoDB to denote the use of a complete stack for development applications using MongoDB, Express, AngularJS and Node.js [43].

- **MongoDB:** It is a powerful and flexible NoSQL database. It combines the ability to scale with the many resources available in relational databases such as indexes, ordering, etc [43]. In the mean

Stack, MongoDB allows you to store and retrieve a data in a format very similar to JavaScript Object Notation (JSON).

- **Express:** It is a light-weight web framework, which helps in organizing your web application in MCV architecture on the server side. Express generally provides REST Endpoints that are consumed by the AngularJS templates, which in turn are updated based on the received data [44].
- **AngularJs:** It is a client-side framework for Single Page Web Applications (SPA) created by Google and released to the public domain in 2009. It greatly simplifies the development, maintenance and testing, as well as facilitating the receipt of data and execution of logic directly on the client. In Mean Stack, it is responsible for dynamic interfaces allowing easy access to REST endpoints directly from the client through specialized services [44].
- **Node.Js:** It is a platform for JavaScript applications created by Dahl under the Chrome JavaScript runtime environment. It is responsible for server-side requests [45].

4.1.2. Android System

Android is the most widely used operating system on smartphones and tablets. It is based on the Linux kernel and currently developed by Google. Android Studio and the Java language was used for the development of the application. Regarding the communication with the Android system the Software Development Kit (SDK) is used, in which it allows the developer to use the functionalities provided by the operating system.

4.2. Functionalities

After the user log in, the app pops up the initial screen with the list of all the evaluations already performed as deployed in Figure 17.

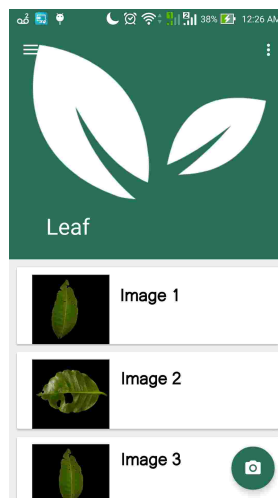


Figure 17: Initial screen with the list of previous classifications.

To re-evaluate, the user clicks on the camera icon of the Figure 17 and then he/she is redirected to the screen deployed in the Figure 18.



Figure 18: Screen showing a coffee leaf to be selected.

After capturing the image, the user must select the region of interest within a grid, so that the leaf is highlighted as shown in Figure 19.

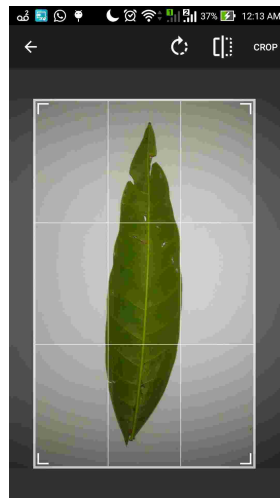


Figure 19: Screen to select the coffee leaf.

After cropping, the image may be uploaded and processed on the server, and the automatic evaluation can be viewed as shown in Figure 20.

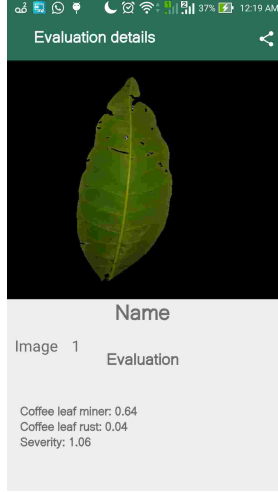


Figure 20: Screen with details of the automatic classification and severity.

5. Conclusion

In this work, we presented the development of a system (an App) that automatically determine the type of coffee leaf disease/pest and the percentage of the injured area. In each process of the development, different approaches have been compared in order to find out the best methods for each case. In image segmentation, the *k-means* algorithm, the Otsu method and the iterative threshold method have been tested on YCgCr color space. For feature extraction attributes of texture and color were calculated. For classification, Artificial Neural Network trained with Backpropagation and Extreme Learning Machine were used. The presented methodology allows an automatic process of classification and calculation of severity of the damaged area of coffee leaves. According to the obtained results in the segmentation, it was clear the importance of choosing the right background to obtain good results. For each chosen background there is a component in the HSV or YCbCr colors space that produce the best result according to the metric used. In general, there is no method or configuration that works well in all cases. In the process of segmentation of damaged foliar area, it was possible to observe more clearly the influence of the background on the leaf color. The camera's automatic adjustment, which depends on the ambient colors, generated images with different shades of green. This had a direct impact on the segmentation of damaged foliar areas of the leaf, which in some images with black or blue background, have generated bad results. For this reason, in this article, the white background is indicated. In the classification process using Artificial Neural Network trained with Backpropagation and Extreme Learning Machine (ELM) good results have been obtained according to the metrics used, but ELM was slightly better. Although the damaged foliar areas of the leaf are noticeably different in color and texture, the good results in the classification show that the attributes chosen were suitable for the this purpose.

The automatic calculation of the severity proposed in this article was compared with the manually using Photoshop by means of the calculation of the injured area and with evaluation of experts and the results

are very close showing the suitability of the approach. Small variations in severity are tolerable in practice, since severity is evaluated in ranges of values. However, the use of backgrounds other than white may generate non consistent results. The next steps for future work is to investigate segmentation methods that are more robust, i.e., that present good results for various types of backgrounds. In addition, we suggest the development of new metrics to evaluate the segmentations and the expansion of the dataset by acquiring more images. As we know there are other diseases and pests that affect coffee leaves. In this case, a deeper study should be made regarding the features extraction and the classifier model. Another point is that with some alterations, the method may be adapted to other plants.

6. Acknowledgements

We gratefully acknowledge the support of NVIDIA Corporation with the donation of the Titan Xp GPU used for this research R.A. Krohling would like to thank the Brazilian agency CNPq and the local Agency of the state of Espirito Santo FAPES for financial support under grant No. 309161/2015-0 and No. 039/2016, respectively.

7. Conflict of Interest Statement

The authors declare that they have no conflicts of interest.

References

References

- [1] H. L. I. d. M. Ventura, J. A.; Costa, Manejo das doenças do cafeeiro conilon, *Café conilon* 2 (2017) 435–479.
- [2] C. L. Garçon, L. Zambolim, E. S. Mizubuti, F. d. Vale, H. Costa, Controle da ferrugem do cafeeiro com base no valor de severidade, *Fitopatologia Brasileira* 29 (5) (2004) 486–549.
- [3] M. J. Fornazier, C. J. Fanton, V. Benassi, D. d. S. MARTINS, Pragas do café conilon, *Café conilon* 1 (2007) 405–449.
- [4] S. Zhang, X. Wu, Z. You, L. Zhang, Leaf image based cucumber disease recognition using sparse representation classification, *Computers and Electronics in Agriculture* 134 (2017) 135–141.
- [5] T. Pahikkala, K. Kari, H. Mattila, A. Lepistö, J. Teuhola, O. S. Nevalainen, E. Tyystjärvi, Classification of plant species from images of overlapping leaves, *Computers and Electronics in Agriculture* 118 (2015) 186–192.
- [6] A. Aakif, M. F. Khan, Automatic classification of plants based on their leaves, *Biosystems Engineering* 139 (2015) 66–75.

- [7] V. Singh, A. Misra, Detection of plant leaf diseases using image segmentation and soft computing techniques, *Information Processing in Agriculture* 4 (1) (2017) 41–49.
- [8] E. Hitimana, O. Gwun, Automatic estimation of live coffee leaf infection based on image processing techniques, *arXiv preprint arXiv:1402.5805*.
- [9] S. P. Patel, A. K. Dewangan, Automatic detection of plant leaf disease using k-means clustering and segmentation, *International Journal of Scientific Research Engineering & Technology* (6) (2017) 774–779.
- [10] A. Rastogi, R. Arora, S. Sharma, Leaf disease detection and grading using computer vision technology & fuzzy logic, *2nd International Conference on Signal Processing and Integrated Networks (SPIN)* (2015) 500–505.
- [11] E. Prasetyo, R. D. Adityo, N. Suciati, C. Fatichah, Mango leaf image segmentation on HSV and YCbCr color spaces using Otsu thresholding, *3rd International Conference on Science and Technology-Computer (ICST)* (2017) 99–103.
- [12] E. Mwebaze, G. Owomugisha, Machine learning for plant disease incidence and severity measurements from leaf images, *15th IEEE International Conference on Machine Learning and Applications (ICMLA)* (2016) 158–163.
- [13] S. P. Mohanty, D. P. Hughes, M. Salathé, Using deep learning for image-based plant disease detection, *Frontiers in plant science* 7 (2016) 1419–1429.
- [14] J. M. Chaves-González, M. A. Vega-Rodríguez, J. A. Gómez-Pulido, J. M. Sánchez-Pérez, Detecting skin in face recognition systems: A colour spaces study, *Digital Signal Processing* 20 (3) (2010) 806–823.
- [15] J. J. De Dios, N. Garcia, Face detection based on a new color space YCgCr, *Proceedings. 2003 International Conference on Image Processing, 2003. ICIP 2003* 3 (2003) III–909.
- [16] K. B. Shaik, P. Ganesan, V. Kalist, B. Sathish, J. M. M. Jenitha, Comparative study of skin color detection and segmentation in HSV and YCbCr color space, *Procedia Computer Science* 57 (2015) 41–48.
- [17] P. Lambert, Filtering and segmentation: The specificity of color images, *International Conference on Color in Graphics and Image Processing-CGIP’2000* (2000) 57–71.
- [18] J. Zhang, J. Hu, Image segmentation based on 2D Otsu method with histogram analysis, *2008 International Conference on Computer Science and Software Engineering* (2008) 105–108.
- [19] D. Liu, J. Yu, Otsu method and k-means, *Ninth International Conference on Hybrid Intelligent Systems. HIS’09*. 1 (2009) 344–349.

- [20] N. Otsu, A threshold selection method from gray-level histograms, *IEEE Transactions on Systems, Man, and Cybernetics* 9 (1) (1979) 62–66.
- [21] J. MacQueen, et al., Some methods for classification and analysis of multivariate observations, in: *Proceedings of the fifth Berkeley symposium on mathematical statistics and probability*, 1967, pp. 281–297.
- [22] K. Wagstaff, C. Cardie, S. Rogers, S. Schrödl, et al., Constrained k-means clustering with background knowledge, *Proceedings of the Eighteenth International Conference on Machine Learning* 1 (2001) 577–584.
- [23] Y. Feng, K. He, A color image based fast segmentation method of crop leaf lesion, *12th IEEE Conference on Industrial Electronics and Applications (ICIEA)* (2017) 116–121.
- [24] J. de Andrade Oliveira, *Classificação de regiões usando atributos de forma e seleção de atributos*, Master’s thesis, Instituto Nacional de Pesquisas Espaciais, São José dos Campos, SP, Brazil (2005).
- [25] J. de Andrade Oliveira, L. V. Dutra, C. D. Rennó, P. S. Santos, Extração de atributos de forma para classificação de imagens de alta resolução do satélite., *Anais XIV Simpósio Brasileiro de Sensoriamento Remoto* (2009) 7015–7022.
- [26] R. M. Haralick, K. Shanmugam, I. Dinstein, et al., Textural features for image classification, *IEEE Transactions on Systems, Man, and Cybernetics* 3 (6) (1973) 610–621.
- [27] J. V. Soares, C. D. Rennó, A. R. Formaggio, C. d. C. F. Yanasse, A. C. Frery, An investigation of the selection of texture features for crop discrimination using SAR imagery, *Remote Sensing of Environment* 59 (2) (1997) 234–247.
- [28] G. Mandloi, A survey on feature extraction techniques for color images, *International Journal of Computer Science and Information Technologies* 5 (3) (2014) 4615–4620.
- [29] D. Monsalve, M. Trujillo, D. Chaves, Automatic classification of nutritional deficiencies in coffee plants, *6th Latin-American Conference on Networked and Electronic Media*.
- [30] C. C. Aggarwal (Ed.), *Data classification: algorithms and applications*, CRC Press, 2014.
- [31] K. L. Priddy, P. E. Keller, *Artificial neural networks: an introduction*, Vol. 68, SPIE press, 2005.
- [32] S. S. Haykin, *Neural networks and learning machines*, Vol. 3, Pearson Upper Saddle River, NJ, USA:, 2009.
- [33] W. S. McCulloch, W. Pitts, A logical calculus of the ideas immanent in nervous activity, *The bulletin of Mathematical Biophysics* 5 (4) (1943) 115–133.

- [34] G.-B. Huang, H. Zhou, X. Ding, R. Zhang, Extreme learning machine for regression and multiclass classification, *IEEE Transactions on Systems, Man, and Cybernetics, Part B (Cybernetics)* 42 (2) (2012) 513–529.
- [35] G.-B. Huang, Q.-Y. Zhu, C.-K. Siew, Extreme learning machine: a new learning scheme of feedforward neural networks, *IEEE International Joint Conference on Neural Networks*, 2004. 2 (2004) 985–990.
- [36] G.-B. Huang, Q.-Y. Zhu, C.-K. Siew, Extreme learning machine: theory and applications, *Neurocomputing* 70 (1-3) (2006) 489–501.
- [37] M. A. Mazurowski, P. A. Habas, J. M. Zurada, J. Y. Lo, J. A. Baker, G. D. Tourassi, Training neural network classifiers for medical decision making: The effects of imbalanced datasets on classification performance, *Neural networks* 21 (2-3) (2008) 427–436.
- [38] G. E. Meyer, J. C. Neto, Verification of color vegetation indices for automated crop imaging applications, *Computers and Electronics in Agriculture* 63 (2) (2008) 282–293.
- [39] D. M. Powers, Evaluation: from precision, recall and F-measure to ROC, informedness, markedness and correlation, *Journal of Machine Learning Technologies* 2 (2011) 37–63.
- [40] L. Bottou, Large-scale machine learning with stochastic gradient descent, *Proceedings of COMPSTAT'2010* (2010) 177–186.
- [41] Y. LeCun, Y. Bengio, G. Hinton, Deep learning, *Nature* 521 (7553) (2015) 436–444.
- [42] J. Baghel, P. Jain, K-means segmentation method for automatic leaf disease detection, *Int. Journal of Engineering Research and Application* 6 (2016) 83–86.
- [43] K. Chodorow, M. Dirolf, *MongoDB: The Definitive Guide* O'Reilly Media, O'Reilly Media, 2010.
- [44] F. Almeida, *Mean: Full stack JavaScript para aplicações web com MongoDB, Express, Angular e Node*, Editora Casa do Código, 2015.
- [45] M. Cantelon, M. Harter, T. Holowaychuk, N. Rajlich, *Node.js in Action*, 1st Edition, Manning Publications Co., Greenwich, CT, USA, 2013.